Published in final edited form as:

Stem Cell Res. 2014 January ; 12(1): 11–23. doi:10.1016/j.scr.2013.09.013.

Hydrogel formulation determines cell fate of fetal and adult neural progenitor cells

Emily R. Aurand[a], **Jennifer L. Wagner**[b], **Robin Shandas**[b], and **Kimberly B. Bjugstad**[a,c]

Emily R. Aurand: Aurand@ucdenver.edu; Jennifer L. Wagner: Jennifer.Wagner@ucdenver.edu; Robin Shandas: Robin.Shandas@ucdenver.edu; Kimberly B. Bjugstad: Kimberly.Bjugstad@ucdenver.edu

[a]Neuroscience Program, University of Colorado, Anschutz Medical Campus, Mail Stop 8313, 12800 E. 19th Avenue, Aurora, CO 80045, USA

[b]Department of Bioengineering, University of Colorado, Anschutz Medical Campus, Mail Stop 8607, 12700 E. 19th Avenue, Aurora, CO 80045, USA

[c]Department of Pediatrics, University of Colorado, Anschutz Medical Campus, Mail Stop 8313, 12800 E. 19th Avenue, Aurora, CO 80045, USA

Abstract

Hydrogels provide a unique tool for neural tissue engineering. These materials can be customized for certain functions, i.e. to provide cell/drug delivery or act as a physical scaffold. Unfortunately, hydrogel complexities can negatively impact their biocompatibility, resulting in unintended consequences. These adverse effects may be combated with a better understanding of hydrogel chemical, physical, and mechanical properties, and how these properties affect encapsulated neural cells. We defined the polymerization and degradation rates and compressive moduli of 25 hydrogels formulated from different concentrations of hyaluronic acid (HA) and poly(ethylene glycol) (PEG). Changes in compressive modulus were driven primarily by the HA concentration. The in vitro biocompatibility of fetal-derived (fNPC) and adult-derived (aNPC) neural progenitor cells was dependent on hydrogel formulation. Acute survival of fNPC benefited from hydrogel encapsulation. NPC differentiation was divergent: fNPC differentiated into mostly glial cells, compared with neuronal differentiation of aNPC. Differentiation was influenced in part by the hydrogel mechanical properties. This study indicates that there can be a wide range of HA and PEG hydrogels compatible with NPC. Additionally, this is the first study comparing hydrogel encapsulation of NPC derived from different aged sources, with data suggesting that fNPC and aNPC respond dissimilarly within the same hydrogel formulation.

Introduction

The high water content and highly customizable nature of hydrogels make these materials well suited for tissue engineering, especially in the brain and spinal cord. Unfortunately, too many studies use hydrogels without reporting the tunable properties. As a consequence, they

Correspondence to: Emily R. Aurand, Aurand@ucdenver.edu.

Supplementary data to this article can be found online at http://dx.doi.org/10.1016/j.scr.2013.09.013.

may not recognize how these properties can alter their final results. Hydrogel chemistry, including the molecular weight (mw) of the components, the type of polymerizing modifications, and the total polymer content, all contribute to the customization of hydrogel behaviors (e.g. the physical properties, such as polymerization and degradation, and the mechanical properties). These behaviors will determine the success of a hydrogel used for tissue engineering. For example, two studies treating spinal cord injury used chemically similar hydrogels but reported substantially different results: Park et al. (2010) found significant repair after spinal cord injury using a hyaluronic acid (HA; mw 170 kDa) hydrogel with an identified shear storage modulus (G′) of 0.3 kPa, but an undefined final weight percent (wt.%) of HA and an unspecific HA modification to allow for polymerization. In contrast, Horn et al. (2007) found no repair of the spinal cord using a thiol-modified HA-based hydrogel at a 0.5 or 1.0 wt.%, but failed to report the molecular weight of the HA or the mechanical properties of the hydrogel. While the hydrogels used in these two studies are very similar in chemistry, neither study provides enough detail about the tunable properties to be independently replicated. Hydrogel chemistry and subsequent physical and mechanical properties all have unique contributions to successful tissue engineering, specifically with regard to the reaction of the host tissue to the hydrogel and how replacement cells respond to hydrogel encapsulation (Aurand et al., 2012a,b). A comprehensive exploration of hydrogels well suited for neural tissue engineering, composed of commercially available materials with defined tunable properties may help standardize the use of hydrogels for neural tissue repair.

Hydrogels comprised of HA and poly(ethylene glycol) (PEG) provide both the natural element (HA) for neural cell interaction and the synthetic element (PEG) for customization and functionalization. HA is the main polymer backbone of the extracellular matrix (ECM) of the brain and is degraded by hyaluronidases produced by both neurons and glia in vivo (Al'Qteishat et al., 2006; Lindwall et al., 2013). Biologically inert PEG provides additional control over hydrogel physical properties and helps to enhance functionality through prefabrication of more complex polymers, allowing for the attachment of cells or incorporation of growth factors or drugs (Aurand et al., 2012a,b; Burdick et al., 2006; Lampe et al., 2011; Lin and Anseth, 2009; Lin et al., 2009, 2011; Sawhney et al., 1993; Young and Engler, 2011). Our study employs only these two components, without further modifications, to assess baseline biocompatibility and explore how changes in hydrogel polymer ratio and subsequent physical and mechanical properties affect the fate of encapsulated neural progenitor cells (NPC).

Many studies have explored the use of neural cells and tissue for their use in treating neurological disorders (Goldman, 2011; Barker et al., 2003; Svendsen et al., 1999). Clinical trials have been undertaken implanting neural stem cells and NPC to treat a number of neurological diseases, including Parkinson's, Batten disease, and cerebral palsy (Gupta et al., 2012; Olanow et al., 2003; Trounson et al., 2011; Selden et al., 2013; Luan et al., 2012). Because of the ethical controversies surrounding the destruction of a fetus, research has also begun to explore the potential use of NPC derived from adult brain (Lo and Parham, 2009; Su et al., 2011). Currently published studies often treat NPC derived from fetal or adult brains as the same type of cells. Indeed, Pollard et al. (2006) found NPC from adult and fetal sources express the same neural progenitor markers (e.g., nestin, sox2, blbp and olig2) and

respond similarly to basic fibroblast growth factor (bFGF) and epidermal growth factor (EGF). While the major molecular NPC qualities are common to both cell types, few studies have compared the fates of these two cell types in vitro and even fewer studies have addressed the fate of hydrogel-encapsulated NPC using cells from either source.

Hydrogel biocompatibility is improved when the mechanical properties of the hydrogel are matched to the host tissue (Aurand et al., 2012a,b; Banerjee et al., 2009; Engler et al., 2006; Georges et al., 2006; Saha et al., 2008; Seidlits et al., 2010; Teixeira et al., 2009). Since tissue-matching is an important quality of a successful hydrogel, we investigated the fate of both fetal- and adult-derived NPC in twenty-five different HA and PEG hydrogels. Because fetal-derived NPC are extracted from a brain with an inherently weaker mechanical integrity than adult-derived NPC, where the brain is stiffer (Elkin et al., 2010), we hypothesized that the survival and differentiation of NPC would be optimal when encapsulated into hydrogels that more closely match the originating tissue. Our study is unique because of this comparison between fetal tissue-derived NPC and adult tissue-derived NPC encapsulated in a range of biologically relevant hydrogels with mechanical properties of both juvenile and adult brain.

Methods

Hydrogel formulations and polymerization

Polymer hydrogels were formulated from thiol-modified carboxy-methylated hyaluronic acid (CMHAS; “HA”) and thiol-reactive poly(ethylene glycol) diacrylate (PEG). Both products were purchased from Glycosan BioSystems, Inc. (Cat.# GS222 and GS700). The HA had a molecular weight of 250 ± 30 kDa and a company-reported degree of methylation of approximately 75–85%; the PEG had a molecular weight of 3.4 kDa and the company has reported a 95% or greater degree of acrylation. Lyophilized HA and PEG solids were reconstituted with degassed, deionized water (DG water; cat# GS241, Glycosan BioSystems, Inc.) to 2%(w/v HA) and 10%(w/v PEG) stock solutions. To achieve the desired formulations in Table 1, additional DG water was added to dilute stock materials as needed. For degradation experiments and mechanical testing, trypan blue was added to the DG water to visualize the hydrogels (final trypan blue concentration <0.00002%). For in vitro experiments, DG water was replaced with Hanks' Balanced Salt Solution (HBSS; Gibco) to improve cytocompatibility with encapsulated cells.

Hydrogels were made in 25 different formulations as based on the final polymer ratios of HA%(w/v) to PEG%(w/v) (Table 1). HA ranged from 0.2% to 1.0% in 0.2% increments and PEG ranged from 0.6% to 3.0% in 0.6% increments. The range of polymer concentrations were chosen based on company instructions for preparations, on achieving a range which encompassed mechanical properties of brain tissue, and on practicality of use. Hydrogels with greater than 1.0% HA and 3.0% PEG polymerized too quickly (<30 s) for practical use. Hydrogels with less than 0.2% HA retained a liquid status, making these materials ineffective at encapsulating cells three-dimensionally or to undergo mechanical testing with the described methods. Hydrogels were formed by adding DG water and stock PEG in discrete volumes to a vial of stock HA. Materials were then transferred via pipette to the respective polymerization vessels. Formulations were made in HA dilution series (i.e. 1.0%

to 0.2%HA) with the PEG concentration kept constant by adding additional stock PEG and DG water to the vial of HA. For example, formulation “A” was made starting with stock HA and adding PEG and DG water to create a 1.0%HA and 3.0%PEG hydrogel solution. Material was removed to the polymerization vessel and additional DG water and PEG were added to the remaining HA to create formulation “F” (0.8%HA:3.0%PEG), and so on until the five formulations using 3.0% PEG were obtained. Volumes varied based on experiment.

Polymerization of the hydrogel materials occurs through covalent bond formation between the thiol modifications on the HA and the thiol-reactive portions of the diacrylated PEG. This reaction is independent of low pH or temperature steps and does not require ultraviolet exposure. The polymerization rate (or gelation time) was determined per manufacturer's instructions and based on published literature (Ambati and Rankin, 2011; Lee et al., 2004; Jin et al., 2012; He et al., 2000; Hudalla et al., 2008). This rate was recorded as the amount of time (in minutes) from the combination of materials to form a solid product as determined by inversion and indentation.

Hydrogel degradation

Hydrogel degradation was measured using the samples from mechanical testing. Each hydrogel sample was quartered and each quarter placed in one well of a 12-well plate containing 1 mL of ~100 U/mL hyaluronidase ((Burdick et al., 2005); cat.# H3506, Sigma-Aldrich) in HBSS. Hydrogels in enzyme solution were incubated in a 37 °C humidified chamber. Half of the degradation solution was replaced every other day, with care taken not to disturb the hydrogel. Hydrogels were observed twice daily for 72-hours and then once daily until complete degradation. Complete degradation was determined as the point at which the hydrogel was no longer visibly present to the naked eye and no solid product could be found in the solution. The time to complete degradation was measured in days.

Mechanical testing

Compressive modulus was used as a measure of hydrogel stiffness. For each formulation, 400 μL of hydrogel solution was polymerized at room temperature in a 10 mm × 10 mm × 4 mm biopsy mold (Electron Microscopy Sciences). Polymerized hydrogels were incubated at 37 °C in a humidified chamber for 24 h prior to testing. Hydrogels were brought to room temperature and extracted from the mold using a thin metal spatula. Hydrogel dimensions were measured to ensure uniform size and for modulus calculations. Testing was done using an MTS Insight 5-SL uni-axial mechanical tester (MTS Systems) fitted with a 5 N load cell. Samples were compressed at a rate of 200 μm/min to an end-strain of 40% of initial height. Compressive modulus (kPa) was calculated as the slope at 20% strain of an exponential fit to a true stress-true strain curve. The curve was constructed from data that was filtered with a sliding average filter, window size five, to reduce noise and truncated to contain values between 0 and 30% strain. Data is presented as the mean ± SEM compressive modulus in kPa of four to six measures (samples) per formulation.

For comparison, brain tissue samples were measured for compressive modulus in a similar manner. Whole brains were extracted immediately following CO2 euthanasia from rat pups (postnatal day 7, n = 3), adult rats (at least two months of age, n = 9), and adult mice (2–3

months, n = 5) into ice cold HBSS. Adult tissue was trimmed to match hydrogel dimensions, resulting in the removal of olfactory bulbs, cerebellum, and dorsal cortex, when necessary; sub-cortical structures were kept intact. Juvenile brains were measured whole. Tissues were brought to room temperature and tested using the same parameters as hydrogel samples.

fNPC derivation

Fetal NPC (fNPC) were derived from embryonic day 15 (e15) rats. Timed pregnant Sprague Dawley females (Harlan Laboratories) were terminally anesthetized and both uterine horns were removed. Embryos from each horn were excised into ice cold Hanks' Balanced Salt Solution (HBSS; Gibco) and decapitated. Mean crown-rump length was 13.74 ± 0.07 mm. Whole brains, minus the olfactory bulbs and cerebella, were washed three times in ice cold HBSS. Tissues were manually dissociated to single cell suspension by using first a 10 mL pipette tip, followed by a 1 mL pipette tip. The cell solution was divided into uncoated Petri dishes with approximately three brains per dish. Cultures were grown in standard serum-free medium (3:1 DMEM/ F12 (Mediatech, Inc./HyClone Laboratories, Inc.), 1× B27 supplement (Life Technologies), 100 U/mL penicillin (Fisher Scientific), 1 μg/mL streptomycin (Fisher Scientific), 2 mM L-glutamine (Fisher Scientific), and 20 ng/mL basic fibroblast growth factor (bFGF) and epidermal growth factor (EGF)) at 37 °C and 5% CO_2. One half of the culture medium was replaced every other day. Six days after plating (DIV6), cells were dissociated and frozen in standard medium with 10% DMSO (Fisher Scientific) and stored in liquid nitrogen. For encapsulation into hydrogels, fNPC were thawed and plated in standard medium in Petri dishes. The fNPC were maintained in dishes for four days prior to encapsulation. To ensure the cells were NPC, a small sample (at least 2000 cells) was plated onto a gelatin coated slide, and immunolabeled for nestin (neural progenitor cell marker), beta-tubulin III (βTubIII; neuronal marker), and glial fibrillary acidic protein (GFAP, glial marker).

aNPC derivation

Adult NPC (aNPC) were generated from the hippocampi and subventricular zones (SVZ) of adult female Sprague Dawley rats. Animals were euthanized by CO_2 asphyxiation and decapitated. Whole brains were removed and the hippocampus was dissected bilaterally into ice cold sterile HBSS. To obtain the SVZ, a coronal section, rostral to the hippocampus and containing the lateral ventricle, striatum, and septum was excised. Using a surgical blade, the striatal and septal tissues were trimmed to approximately 3 mm from the lateral ventricle on all sides to isolate the ependymal and subependymal layers of the ventricle. All tissues were combined, cut into smaller pieces, and washed three times in sterile HBSS. Tissue pieces were manually dissociated to a cell solution with a 10 mL pipette tip, followed by a 1 mL pipette tip. This cell solution was split into uncoated Petri dishes (2–3 brains per dish) and cells were cultured in standard medium as described for fNPC. Every other day, one half of the medium was replaced from the top of the dish. Cells were cultured at 37 °C and 5% CO_2 for 25 days (DIV25) and aNPC were allowed to attach to the dish. At DIV25 cells were collected, manually dissociated, and frozen in standard medium with 10% DMSO and stored in liquid nitrogen. For encapsulation into hydrogels, aNPC were thawed and plated into standard medium in Petri dishes. The aNPC were maintained in dishes for four days prior to

encapsulation. As with the fNPC, a sample of aNPC was immunolabeled for nestin, βTubIII, and GFAP.

NPC encapsulation

NPC were encapsulated at DIV10 for fNPC and DIV29 for aNPC. For aNPC, attached cells were dissociated from the petri dishes using a cell scraper; fNPC were collected as floating neurospheres. All NPC were collected into a 15 mL tube and washed in HBSS. NPC were then manually dissociated to single cell solution by gently pipetting using a 200 μL pipette tip. Cells were re-suspended in HBSS at a concentration of 10,000 viable cells (vc)/μL. For NPC encapsulation, hydrogels were fabricated in a manner similar to those used for mechanical testing, except cell solution and additional HBSS were used in place of DG H_2O. Cell solution was combined with reconstituted HA prior to addition of PEG and gently vortexed, to ensure even three-dimensional (3D) encapsulation. Hydrogel series were made by adding additional cell solution, HBSS, and PEG to achieve the desired hydrogel formulation (Table 1) with a final concentration of 1000 vc/μL for each hydrogel sample.

NPC 24-hour survival

NPC survival was assessed 24 h post-encapsulation. Fetal or adult NPC were encapsulated into the hydrogels as described. A 96-well plate was used to polymerize 50 μL of hydrogel-cell material per well, with four to eight wells per formulation for fNPC and three to eight wells per formulation for aNPC. Hydrogels were allowed to polymerize fully for approximately 40 min before 100 μL of standard medium was added to each well. As a control, wells with 50 μL of dissociated NPC alone (1000 vc/μL) in standard medium were also cultured (TCP controls; n = 9). The approximate cell density, based on the surface area of TCP wells, was 1562 vc/mm^2. Plates were incubated for 24 h at 37 °C and 5% CO_2. The MultiTox-Fluor Multiplex Cytotoxicity Assay (Promega, cat.#G9200, Madison, WI) was used to measure cell viability per manufacturer's instructions. Medium was removed from atop the hydrogel and hydrogels were incubated with 50 μL assay reagent for 3 h at 37 °C. Control wells and a cell curve (50 μL per well, fNPC or aNPC cultured the day of measurements) were incubated with 50 μL of assay reagent for 30 min. Hydrogels were incubated longer to allow reagent to fully permeate the hydrogel, but within the time frame suggested by the manufacturer. Live cell fluorescence was measured using a Bioteck Synergy HT multi-modal microplate reader at 400 nm excitation and 508 nm emission. Data from all reads were combined by formulation and total cell numbers were determined using an averaged cell curve. Any outliers, as determined by the statistical software, were excluded from the analysis; outliers were rare and excluded 3 of 148 data points for fNPC and 7 of 104 data points for aNPC. Total cell numbers, representing survival, were calculated in a volume of 50 μL.

Cell numbers and differentiation at three weeks

To determine the long-term effects of hydrogel encapsulation on cell number and differentiation, a low density of NPC were cultured for three-weeks in serum-based media to drive differentiation. This lower density was chosen to limit the influence of cell-to-cell factors driving differentiation, enhancing the influence of the hydrogel. To do this, CultureWell™ multiwell chambered coverslips (Grace BioLabs, item# 103380; Bend, OR)

were coated with 15 μg/mL poly-L-ornithine and incubated at 37 °C overnight, at which time remaining poly-L-ornithine was aspirated off. Coverslips were washed three-times with HBSS and air dried. Twenty microliters of hydrogel solution containing NPC (1000 vc/μL) was added to each well and allowed to polymerize at 37 °C for approximately 40 min. As a control, 20 μL of unencapsulated NPC solution was also plated directly onto the coverslip (TCP control). Chambered coverslips were placed in 100 mm petri dishes (2 per dish) and dishes were filled with differentiation medium (1:1 DMEM/F12, 100 U/mL penicillin, 1 μg/mL streptomycin, 2 mM L-glutamine, and 10% fetal bovine serum (FBS; Fisher Scientific, Fair Lawn, NJ)). Plates were incubated at 37 °C and 5% CO_2. No additional growth factors were added to direct NPC differentiation towards a specific cell fate. Half of the differentiation medium was replaced every other day. After three weeks, cells were fixed with 4% paraformaldehyde and processed for immunocytochemistry. Each hydrogel-NPC formulation and unencapsulated TCP controls had 3–4 wells. Based on the surface area of the TCP controls, the cell density was 707 vc/mm^2, approximately half the cell density of the 24 hour cultures.

Immunocytochemistry and microscopy

To identify NPC that either differentiated into astrocytes, neurons, or remained undifferentiated, all chambered coverslips were processed for immunocytochemistry (ICC). Standard ICC methods were followed except that washes and incubation periods were extended to assure materials penetrated the hydrogels. All washes were done in PBS three times for 10–20 min each. Each well was incubated in protein block (5% goat serum, 1% bovine serum albumin, and 0.3% Triton X-100 in PBS) for 2 h. To label astrocytes, anti-glial fibrillary acidic protein (GFAP; rabbit anti-GFAP; Zymed Laboratories, Carlsbad, CA, Cat# 18–0063; 1:500) was used and wells were incubated overnight at 4 °C. The next day a Cy-3 goat anti-rabbit secondary antibody was used (Jackson ImmunoResearch Laboratories, West Grove, PA, Cat# 11-165-144; 1:400) and wells were incubated for 4 h at room temperature in the dark. To label neurons, anti-beta tubulin III (rabbit anti-β-tubulin III), conjugated to Alexa Fluor 488 (βTubIII; Millipore, Temecula, CA, Cat# AB15708A4; 1:400) was used and incubated overnight at 4 °C. All cell nuclei were labeled with 4′,6-diamidino-2-phenylindole (DAPI; Fisher Scientific, Fair Lawn, NJ) at 100 ng/mL in PBS for 1 h at room temperature, followed by one wash overnight in PBS at 4 °C. Following ICC, coverslips were removed from the petri dishes and placed on glass slides with anti-fade mounting medium (0.1 M propyl gallate in 9:1 glycerol/PBS).

An Olympus BX61 microscope complete image analysis system with CellSens suite image analysis software was used to create images of hydrogels and TCP control wells. Z-stacks were made of hydrogels with a height greater than 7 μm. Four images (most of which were stacked images) were taken per well.

To assess the number of cells still present at three weeks post-encapsulation, the total number of DAPI+ cells was counted per image. The use of DAPI at this time point allowed us to identify the total numbers of whole and intact cells still incorporated into the hydrogel. The number of DAPI positive cells was used to determine the average density of cells per mm^3 for hydrogels or mm^2 for TCP controls. The average density was multiplied by the

total volume (with remaining hydrogel height given by the Z-stack) or surface area of each well to achieve a total number of cells for the well. Data are reported as the mean total number of cells by formulation.

To assess differentiation, cells in each image were counted as either GFAP+ (glia/astrocytes), βTubIII+ (neurons), or as GFAP and βTubIII negative (undifferentiated NPC), resulting in three outcome groups ("cell types"). Cell populations were determined as a density of cells per mm^3 volume of hydrogel, with hydrogel height given by the Z stack. Differentiation data are reported as a percent of the total cells counted.

Data analysis and statistics

All data were analyzed using the Statistica software (Statistica 7.0, Statsoft, Inc.). Two-way ANOVAs were used to compare levels of HA, levels of PEG, and the interaction between HA and PEG, on the rates of polymerization, degradation, mechanical properties, and NPC survival. NPC differentiation was analyzed using a 3-way ANOVA with cell types as a repeated measure. Individual cell counts for survival and differentiation were correlated with mean compressive modulus for each formulation. Fetal NPC and adult NPC were analyzed separately. When significant differences were found, a Fisher Least Significant Difference post-hoc test was used to identify differences between specific means. Significance was determined at $p < 0.05$. Data were graphed as color-coded contour graphs for interactions between HA and PEG. The levels of HA were plotted on the x-axis, the levels of PEG on the y-axis, and the measured data are represented in the contours of the z-axis. Contours were derived from the raw data using a distance-weighted least squares calculation.

Results

Polymerization

Polymerization rate was measured as the number of minutes required for a hydrogel formulation to solidify, as indicated by the inversion method. Polymerization rates ranged from 2 to 40 min. Hydrogels containing less than 0.4% HA were excluded from the statistical analysis because they failed to form a solid product. There was a significant effect of HA content ($F(3, 50) = 40.90$, $p < 0.0001$), as well as PEG content ($F(4, 50) = 15.43$, $p < 0.0001$), on the polymerization rate. When either HA or PEG content in the hydrogels was increased, the polymerization rate increased (occurred more quickly) (Fig. 1A). There was no significant interaction between the HA and PEG on polymerization rates ($F(12, 50) = 1.58$, $p > 0.05$), suggesting that they both contributed to polymerization, but their effects were not additive.

Degradation

Hydrogels were subjected to enzymatic degradation in a hyaluronidase solution. While not necessarily reflective of in vivo degradation or that initiated by cells in vitro, this was done to determine a relative timeline of degradation. Degradation rates ranged from less than 12 h (0.5 days) to 12 days. Conversely to the polymerization rates, increasing the HA content significantly decreased degradation rate ($F(4, 87) = 370.39$, $p < 0.0001$), as did increasing the PEG content ($F(4, 87) = 101.94$, $p < 0.0001$). There was also a significant interaction

between HA and PEG content ($F(16, 87) = 40.50$, $p < 0.0001$) (Fig. 1B). At low levels of HA (0.2% and 0.4%), none of the PEG contents tested changed the degradation rate. However, as HA content increased, higher levels of PEG (1.8%, 2.4%, and 3.0%) substantially slowed degradation. Therefore, the degradation rates of hydrogels with HA content of 0.8% and 1.0% could be manipulated by altering the PEG content.

Compressive modulus

Compressive modulus was measured in kPa. Hydrogels had a mean range from 0.12 ± 0.06 kPa to 31.30 ± 1.92 kPa, with an average compressive modulus of 9.40 ± 0.90 kPa. These measures overlapped the measures of fresh brain tissue (Table 2). In brain tissue, the compressive modulus varied based on species and age. In general, rats had a higher compressive modulus than mice of the same age. Furthermore, brains from older rats (≥2 months) also had a higher compressive modulus than brains from young rats (post-natal day 7).

For the hydrogels, compressive modulus was significantly influenced by HA, with a modulating effect by PEG content (Fig. 2). Overall, as HA content increased, there was a corresponding increase in the compressive modulus ($F(4, 86) = 115.43$, $p < 0.0001$). Likewise, as PEG content was increased, there was an increase in the compressive modulus ($F(4, 86) = 19.16$, $p < 0.0001$). Similar to degradation, the combined effect of HA and PEG significantly altered compressive modulus ($F(16, 86) = 5.60$, $p < 0.0001$). At low levels of HA, increasing levels of PEG had a minimal effect on compressive modulus ($p > 0.05$). However, at the higher levels of HA (0.6%, 0.8%, and 1.0%), increased PEG content significantly enhanced the increase in compressive modulus ($p < 0.05$). Thus, like degradation, hydrogels with HA content of 0.8% and 1.0% were the most amenable to manipulating the compressive modulus, simply by changing the PEG content.

fNPC survival and differentiation

Fetal NPC (fNPC) survival was measured 24 h post-encapsulation. Cells encapsulated in hydrogels, regardless of formulation, survived better than unencapsulated fNPC in TCP controls (mean survival for all 25 hydrogels = 61137.66 ± 1346.63; mean TCP survival = 17311.75 ± 1736.67). Comparisons between the 25 hydrogels indicate that survival of hydrogel-encapsulated fNPC was increased as HA content increased ($F(4, 120) = 78.97$, $p < 0.0001$), but decreased when PEG content was increased ($F(4, 120) = 281.71$, $p < 0.0001$). The combined effects of both HA and PEG created a significant interaction ($F(16, 120) = 47.54$, $p < 0.0001$). At the highest concentration of HA (1.0%), survival rates were fairly consistent regardless of the amount of PEG. As HA content decreased, the amount of PEG in the hydrogel had a more variable effect, with the lowest survival rates measured in those hydrogels with 2.4% and 3.0% PEG (Fig. 3A).

A correlation between compressive modulus and survival was used to address how the mechanical properties of a hydrogel affect biocompatibility. At 24 h, the hydrogel compressive modulus appeared not to affect the survival of fNPC ($r = 0.22$, $p > 0.05$, $n = 25$), suggesting cell survival at this time-point is dependent on the hydrogel composition and not the relative stiffness.

The persistence of cells encapsulated in the hydrogel was also measured at three weeks post-encapsulation in conditions supporting NPC differentiation. The long-term cell number and degree of differentiation for fNPC and aNPC in hydrogels containing less than 0.4% HA were excluded from the statistical analysis because they did not form a solid hydrogel. These hydrogels degraded too quickly, preventing accurate measurement of outcomes in the described culture conditions.

Results from remaining hydrogels suggest that during this period, the number of fNPC retained within the hydrogels was decreased compared with TCP controls (mean hydrogel cell number = 3627.33 ± 198.83; mean TCP cell number = 24851.59 ± 2718.65). The mean number of persisting cells in the hydrogels was approximately 14% of that in TCP. Across the different hydrogel compositions, the long-term cell retention was impacted by both HA and PEG ($F(3,54) = 3.66$ and $F(4,54) = 22.04$, respectively, $p < 0.05$) and by the interaction between the two hydrogel components ($F(12,54) = 5.30$, $p < 0.0001$). The number of fNPC still present was highest when lower concentrations of HA were paired with higher concentrations of PEG, achieving cell numbers that were 20–25% of that measured in TCP (Fig. 3B). This interaction between HA and PEG is in contrast to cell numbers measured at 24 h, where low HA and high PEG had lower cell numbers. The long-term persistence of fNPC within the hydrogels did not correlate with the compressive modulus ($r = -0.09$, $p > 0.05$, $n = 20$).

The differentiation of fNPC into young neurons and/or astrocytes was assessed at three weeks. The percentage of neuronal cells (βTubIII+), glial cells (GFAP+), or undifferentiated cells (DAPI+, βTubIII- and GFAP-) in each hydrogel was determined. Prior to encapsulation, the cells were consistently >99% nestin-positive and only 1–5 cells were ever found to be positive for βTubIII or GFAP (Suppl. Figs. 1A–C). After three weeks in differentiation medium, many cells differentiated within the hydrogel. Neuronal βTubIII+ cells were the smallest population at 2.80 ± 0.54%, GFAP+ cells comprised an average of 21.14 ± 1.31%, and undifferentiated cells comprised the remaining 76.06 ± 1.32%. The TCP controls, while similar, had slightly fewer βTubIII+ and GFAP+ cells, at 1.34 ± 0.10% and 19.38 ± 1.08% respectively, while most cells (79.28 ± 1.04%) were not positive for either differentiation marker.

Hydrogel formulation had significant effects on fNPC differentiation ($F(24,108) = 2.51$, $p = 0.0007$). Most cells which differentiated expressed GFAP (21.14 ± 1.31%) (Fig. 4A). The percent of glial cells ranged from less-than 10% to almost 40% of the total cell populations. Increases in GFAP+ cell density was mostly measured in hydrogels with the mid-range levels of HA and lower levels of PEG, although a small peak of GFAP+ cells were seen in the hydrogels with 1.0% HA and 3.0% PEG (“A” in Table 1). Neuronal cells made up less than 6% of cells in most hydrogel formulations, with the exception of the 0.4% HA and 1.2% PEG hydrogel (“S” in Table 1; Fig. 4B). In this hydrogel, βTubIII+ cells made up 14.46 ± 1.98% of the population. This increase in neuronal differentiation in hydrogel “S” compared to overall neuronal means (14.46% vs. 2.80% respectively) appears to have occurred at the cost of cells differentiating into glial cells (7.93% vs. 21.14%) rather than a decrease in the overall number of cells which remained undifferentiated (77.61% vs. 76.06%; Fig. 4C).

For fNPC, population changes in glial cell density were related to changes in the hydrogel stiffness. GFAP+ cells increased with increasing compressive modulus ($r = 0.52$, $p < 0.05$, $n = 20$). The differentiation into βTubIII+ cells was not influenced by this mechanical property ($r = -0.25$, $p > 0.05$, $n = 20$).

aNPC survival and differentiation

Overall, hydrogel encapsulation did not improve the 24-hour survival of aNPC compared with TCP controls (mean hydrogel survival = 93884.68 ± 3031.04; mean TCP survival = 130485.22 ± 13027.96). Most hydrogels had fewer surviving aNPC at 24 h than TCP. Within the hydrogel groups alone, there were significant effects of both HA ($F(4,72) = 9.44$, $p < 0.0001$) and PEG ($F(4, 72) = 41.79$, $p < 0.0001$), as well as a combined effect of HA and PEG ($F(16,72) = 5.11$, $p < 0.0001$). Generally, the greatest effects on survival were measured with increased PEG content which significantly decreased survival (Fig. 5A). Increases in HA content also decreased survival, especially at higher PEG concentrations (1.8–3.0% PEG). The most optimal acute survival conditions were measured in hydrogels with both low HA and PEG concentrations. However, there was an independent peak in survival observed in hydrogels with 0.2% HA and 2.4% PEG (“V” in Table 1). Like fNPC, the survival of aNPC at 24 h was not correlated to hydrogel compressive modulus ($r = -0.36$, $p > 0.05$, $n = 25$).

At three weeks, the number of aNPC remaining in some hydrogel formulations was better than that of the TCP controls while some were below control measures (mean hydrogel cell number = 5177.48 ± 383.27; mean TCP cell number = 6104.01 ± 809.90). Comparing the hydrogel formulations, significant interactive effects of both HA and PEG were found on the number of persisting cells at three weeks ($F(12,59) = 4.12$, $p = 0.0001$). At higher concentrations of PEG, long-term cell numbers increased, especially with accompanying increases in HA content. The highest cell numbers were measured in hydrogels with 0.8% HA and 1.8% and 2.4% PEG, and were nearly twice that measured in TCP (Fig. 5B). In general, hydrogels with the lowest amounts of PEG (0.6% and 1.2%) had long-term aNPC cell numbers below TCP controls. This effect was seen regardless of HA content. Unlike the long-term cell numbers of fNPC, the number of aNPC at three weeks was positively correlated with hydrogel mechanical properties. Within the compressive modulus range we measured, as hydrogel compressive modulus increased, there was an increase in the number of aNPC ($r = 0.56$, $p < 0.05$, $n = 20$).

As with the fNPC, prior to encapsulation, >99% of cells were found to be nestin-positive with only 2–3 cells positive for either βTubIII or GFAP (Suppl. Figs. 1D–E). After three weeks exposed to conditions which induce differentiation, the majority of encapsulated aNPC remained undifferentiated (80.02 ± 2.12%), 17.87 ± 1.87% expressed βTubIII, and only 2.11 ± 0.40% expressed GFAP. By comparison, the TCP controls had a differentiation rate of 30.45 ± 2.35% for undifferentiated cells, while 66.30 ± 2.04% of cells expressed βTubIII, and 3.25 ± 1.14% expressed GFAP. The level of overall differentiation in aNPC is consistent with that observed with encapsulated fNPC, however the cell fates (βTubIII vs. GFAP) are in sharp contrast to fNPC, where most differentiated cells were GFAP+.

When considering the effects of the hydrogel composition, HA and PEG had a significant combined effect on aNPC differentiation ($F(24,118) = 11.54$, $p < 0.0001$). Overall, as HA concentration decreased, more cells were found to express GFAP and βTubIII (Figs. 6A and B), however, as both HA and PEG increased, cells remained undifferentiated (negative for βTubIII and GFAP; Fig. 6C). The highest levels of overall differentiation were measured in hydrogels with 0.4% HA and 1.2% PEG ("S" in Table 1), with 50.37 ± 3.16% of cells expressing βTubIII, 13.91 ± 1.02% expressing GFAP, and only 35.72 ± 3.50% appearing to remain in their progenitor state, a rate similar to that observed in TCP controls. An elevated number of βTubIII cells (57.02 ± 3.16%) were also found in hydrogels with 0.4% HA and 3.0% PEG ("P" in Table 1). In this particular formulation though, there was no increase in GFAP+ cells, suggesting a formulation which favors neuronal differentiation rather than general cell maturation.

In aNPC, the compressive modulus was correlated with βTubIII + cell density ($r = -0.68$, $p < 0.05$, $n = 20$) but not GFAP+ cell density ($r = -0.37$, $p > 0.05$, $n = 20$). The negative correlation between βTubIII expression and compressive modulus suggests that aNPC tend to differentiate into neurons on hydrogels which are less stiff.

Discussion and conclusions

Discussion

Our results indicate that there are multiple variables that can affect the interactions between hydrogel and NPC, and the choice of which hydrogel to use is dependent on the function to which the hydrogel will be applied. Both HA and PEG made contributions to polymerization and degradation rates, cell survival, and cell differentiation. Interestingly, HA was the main contributor to compressive modulus, whereas PEG provided slight modifying changes. Furthermore, the impacts of HA and PEG on cell fate were often determined by the age of the neural progenitor donor tissue.

Acute hydrogel biocompatibility, as measured by 24-hour survival, indicated that fetal-derived NPC survived hydrogel encapsulation well. This may be a result of greater plasticity found in fetal-derived cells (Cayre et al., 2009; Gage, 2000; Seaberg et al., 2005). Greater plasticity could allow fNPC to equilibrate more quickly to an environment which more closely resembles developing neural tissue. Alternatively, fNPC may adapt more quickly to the hydrogels because this environment is similar to the neurosphere formations that these cells adopted when cultured prior to encapsulation. Meanwhile, the aNPC prior to encapsulation attached as individual cells to the TCP surface and thus, *initially*, fewer cells may adapt to the 3D hydrogel environment. Adult-derived NPC survival was dependent on the hydrogel formulation, and was generally lower at 24 h than tissue culture controls. In general, however, both cell types appeared to show better survival at 24 h in hydrogels with lower polymer content (Figs. 3A and 5A).

At three weeks, cell numbers were reversed, with fNPC encapsulated in hydrogels markedly lower than in controls and retention of encapsulated aNPC in some hydrogels better than control cell numbers. The effects of hydrogel composition at three weeks were also reversed. Unlike the 24-hour survival, long-term persistence of encapsulated fNPC and aNPC

suggests that both cell types were retained well within hydrogels with higher polymer concentrations, especially the aNPC (Figs. 3B and 5B).

The differences between 24-hour survival and three-week cell numbers could result from the initial polymerization process negatively affecting the aNPC and/or long-term habituation to the microenvironment affecting the fNPC. For example, studies using mouse embryonic fibroblasts encapsulated in HA and PEG hydrogels found that there was significant cell loss *immediately* after encapsulation (Burdick et al., 2005; Yeh et al., 2006). These researchers attribute the cell loss to the polymerization of polymer hydrogel components. This polymerization process could account for the low cell numbers in the aNPC-hydrogel complexes at 24 h. The increased plasticity of the fNPC may have protected these cells from the polymerization process (Cayre et al., 2009; Gage, 2000; Seaberg et al., 2005).

After the initial polymerization process ends, the qualities of the microenvironment likely determine the long-term presence of the cells. We found that increased stiffness of the hydrogel was associated with increased cell numbers at three weeks. This may suggest that, once polymerized, hydrogels with greater polymer content provide a more favorable microenvironment, either by supporting long-term cell survival or supporting the retention of cells in the hydrogel. This microenvironment may be more favorable simply because it provides good structural support while still allowing for the diffusion of nutrients and wastes. The diffusion of solutes in a hydrogel, or in the brain extracellular matrix, is determined by the distance between the crosslinked polymers (Kuntz and Saltzman, 1997). Smaller molecules pass more easily through the crosslinks, whereas larger molecules or cells can be entrapped. Over time, encapsulated cells can modify their microenvironment in vitro through the expression of native ECM proteins and hyaluronidases (Chung et al., 2009; Chung and Burdick, 2009; Muir, 1994; Stabenfeldt et al., 2010). This cell guided restructuring of the hydrogel environment could also permit the pooling and binding of pro-survival growth factors in the medium and secreted from encapsulated cells (Bonneh-Barkay and Wiley, 2009). This environmental restructuring may also provide the NPC with cues for proliferation and/or differentiation (Bonneh-Barkay and Wiley, 2009; Chodobski et al., 2003; Fainstein et al., 2013; Riquelme et al., 2008; Taipale and Keski-Oja, 1997).

One particular cue, contact mediated inhibition of cell growth, may account for the differences in cell numbers between the TCP and the hydrogels at three weeks when using fNPC. Our data suggests that there was greater long-term persistence of the fNPC in the TCP compared to those encapsulated in the hydrogels. Since proliferation is generally guided by cell contact, the low cell density at which the TCP cells were grown could have induced a level of proliferation not found in the hydrogel grown cells. The cells encapsulated into the hydrogel may have undergone contact mediated inhibition due to the 3D nature of their environment.

Additionally, while fNPC in the TCP controls showed an increase in cell number over the three-week culture period (mean cell number is approximately 124% of the starting cell number), fNPC in the hydrogels reached approximately 18% of the starting population. This could be due to cell death, indicating a lack of support provided by the hydrogels, or a release of cells over time from the degrading hydrogel. In the latter scenario, surviving cells

may have been freed from encapsulation as the hydrogel degraded and removed from culture during media changes, resulting in the decrease in cell number. This process may also be the case with the aNPC after three weeks, as suggested by the observance that there were greater cell numbers in hydrogels which degrade more slowly. The addition of modified gelatin, denatured collagen, or other attachment factors might have prevented this cell loss. These additions are often used in studies in which cells are grown *on the surface* of the HA and PEG hydrogels (Shu et al., 2002, 2004, 2006). However, because collagen is not typically found in the brain ECM (Bonneh-Barkay and Wiley, 2009; Bellail et al., 2004; Rauch, 2004; Ruoslahti, 1996), and because we wanted to address baseline biocompatibility of the most basic hydrogel, we did not include additional attachment factors. Future studies will inevitably decide to add factors to customize the hydrogel to improve cellular attachment and/or cell survival. The current study, has allowed a foundation from which that customization can occur with confidence.

Following the encapsulation of undifferentiated nestinpositive cells, we initiated the differentiation of fetal- and adult-derived NPC using serum-supplemented medium. These conditions were free of additional trophic factors that can guide cell fate, such as retinoic acid or ciliary neurotrophic factor (CNTF), which are used to induce neurons and astrocytes respectively (Saha et al., 2008; Chojnacki and Weiss, 2008). Thus, the differentiation of our cells was determined by fundamental properties of the basic hydrogel and cell-intrinsic mechanisms (Kazanis et al., 2010).

Fundamental attributes of the hydrogel, such as the mechanical properties, are known to drive cell fate (Aurand et al., 2012b; Engler et al., 2006; Georges et al., 2006; Saha et al., 2008; Seidlits et al., 2010; Bischofs and Schwarz, 2003; Lampe et al., 2010). For example, mechanical properties that best mimic the nature of brain tissue have been found to induce neuronal differentiation in mesenchymal stem cells and embryonic stem cells (Engler et al., 2006; Keung et al., 2012). In committed neurons and astrocytes, hydrogel stiffness can alter cell morphology, inducing neuritic branching from neurons grown on softer hydrogels and supporting the multi-processed morphology of astrocytes when grown on harder substrates (Georges et al., 2006; Balgude et al., 2001). Most of our cells from both fNPC and aNPC remained undifferentiated (Figs. 4C and 6C). The incomplete state of differentiation is consistent with the previous results in both hydrogels and standard tissue culture conditions (Banerjee et al., 2009; Saha et al., 2008; Seidlits et al., 2010; Conti et al., 2005; Song et al., 2002a,b). Nonetheless, depending on hydrogel formulation, we observed a mixture of neuronal and glial differentiation in both fNPC and aNPC (Figs. 4 and 6). We also observed a mixture of differentiated cell morphologies (Supplemental Fig. 2). Most of the βTubIII+ fetal-derived cells had a more mature neuronal phenotype with neuritic branching (Supplemental Figs. 2A, B), in contrast with the βTubIII+ adult-derived cells in which the labeling was mostly compact and cytoplasmic (Supplemental Figs. 2E, F). GFAP+ cells from both sources showed more mature phenotypes, also indicated by branching, especially the adult-derived cells (Supplemental Figs. 2C, D, and F).

The three-week differentiation of fNPC revealed that GFAP+ cells were the dominant cell type in all hydrogels, but in hydrogels with a compressive modulus that approached adult brain tissue measures, this glial differentiation substantially increased (Fig. 4A). There was

also an increased neuronal differentiation in a small subset of hydrogels with a low compressive modulus, closer to that observed for juvenile brain tissue (Table 2). Our results confirm what Seidlits et al. (2010) also reported. While their data were not quantified, they reported an increase in neuronal differentiation in fNPC encapsulated in hydrogels that match the mechanical properties of fetal brain, and an increase in GFAP+ cells in those hydrogels representative of adult brain (Seidlits et al., 2010).

In contrast, our aNPC had a greater tendency to differentiate into neurons than the fNPC, specifically in hydrogels that had compressive moduli similar to both adult and juvenile brain tissue (Fig. 6). The hydrogel results are consistent with previous findings using adult-derived NPC (Banerjee et al., 2009; Saha et al., 2008). The findings reported by Saha et al. (2008), are interesting because they compared not only mechanical properties of the biomaterials, but also the effects of differentiation media. Using media designed to induce neuronal differentiation, they found that only 40% of their cells expressed beta-tubulin III on hydrogels with an elastic modulus similar to adult brain tissue. This was similar to the levels measured in their tissue culture plates. By comparison, using a standard serum-based medium, similar to that used here, Saha, et al. were able to increase the number of beta-tubulin III-expressing cells to 60% or greater, and reduce the expression of GFAP-positive cells to below 30% on hydrogels with mechanical properties similar to adult and fetal brain tissue. Their study suggests that adult-derived NPC may be susceptible to both mechanical and chemical cues for neuronal differentiation. Our study reveals the contrastive differentiation profiles of the fetal-derived and adult-derived NPC, suggesting that these two cell types are not interchangeable for neural tissue repair applications. This further confirms the impact of hydrogel mechanical properties on encapsulated cell fate and emphasizes the need to select hydrogels for more than just their chemical biocompatibility.

Interestingly, both NPC populations had the highest levels of neuronal differentiation when grown in hydrogels with 0.4% HA and 1.2% PEG (formulation “S”; Figs. 4B and 6B). This differentiation may likely occur because this ratio of HA and PEG produces an ideal chemical, physical, and mechanical environment to support neural differentiation in both fNPC and aNPC. The “S” formulation may be an excellent “introductory” hydrogel for those interested in entering the field of neural tissue engineering. Alternatively, for studies desiring specific cell fates, such as the development of astrocytes for spinal cord repair (Noble et al., 2011), hydrogels “N” or “I” encapsulating fetal-derived NPC may provide the researcher with the desired astrocytic cell type. However, driving differentiation of complete cell populations will require more than simply changing the mechanical properties and picking the right cell source.

Conclusions

This study has established some of the basic properties and biocompatibility for twenty-five hydrogel compositions using various combined levels of HA and PEG in order to identify basic hydrogels suitable for neural tissue engineering. We further explored the contribution of these hydrogels to the fates of encapsulated NPC derived from fetal and adult brain. Now that the primary qualities have been defined for the basic HA and PEG hydrogel, the next step will be to functionalize these hydrogels for a specific purpose. This can be done by

either passively or actively incorporating factors into the hydrogel, through the addition of attachment factors or immune-modulators, or by producing specific geometries to guide cell morphology (Aurand et al., 2012b).

Supplementary Material

Refer to Web version on PubMed Central for supplementary material.

Acknowledgments

The authors would like to acknowledge Kyle Lampe, Ph.D., Craig Lanning, M.S., Connie Brindley, MS, CVT, Sandra Martin, Ph.D., and John R. Sladek, Jr., Ph.D. for their assistance. Funding was provided by the Linda Crnic Institute (K.B.B.) and the Dean's Academic Enrichment Fund, University of Colorado — Anschutz Medical Campus (E.R.A.).

References

Park J, et al. Nerve regeneration following spinal cord injury using matrix metalloproteinase-sensitive, hyaluronic acid-based biomimetic hydrogel scaffold containing brain-derived neurotrophic factor. J. Biomed. Mater. Res. A. 2010; 93A(3):1091–1099. [PubMed: 19768787]

Horn EM, et al. Influence of cross-linked hyaluronic acid hydrogels on neurite outgrowth and recovery from spinal cord injury. J. Neurosurg. Spine. 2007; 6(2):133–140. [PubMed: 17330580]

Aurand E, et al. Building biocompatible hydrogels for tissue engineering of the brain and spinal cord. J. Funct. Biomater. 2012a; 3(4):839–863. [PubMed: 24955749]

Aurand ER, Lampe KJ, Bjugstad KB. Defining and designing polymers and hydrogels for neural tissue engineering. Neurosci. Res. 2012b; 72(3):199–213. [PubMed: 22192467]

Al'Qteishat A, et al. Changes in hyaluronan production and metabolism following ischaemic stroke in man. Brain. 2006; 129(8):2158–2176. [PubMed: 16731541]

Lindwall C, et al. Selective expression of hyaluronan and receptor for hyaluronan mediated motility (Rhamm) in the adult mouse subventricular zone and rostral migratory stream and in ischemic cortex. Brain Res. 2013; 1503:62–77. [PubMed: 23391595]

Burdick JA, et al. Stimulation of neurite outgrowth by neurotrophins delivered from degradable hydrogels. Biomaterials. 2006; 27(3):452–459. [PubMed: 16115674]

Lampe KJ, et al. The administration of BDNF and GDNF to the brain via PLGA microparticles patterned within a degradable PEG-based hydrogel: Protein distribution and the glial response. J. Biomed. Mater. Res. A. 2011; 96A(3):595–607. [PubMed: 21254391]

Lin CC, Anseth KS. PEG hydrogels for the controlled release of biomolecules in regenerative medicine. Pharm. Res. 2009; 26(3):631–643. [PubMed: 19089601]

Lin C-C, Metters AT, Anseth KS. Functional PEG-peptide hydrogels to modulate local inflammation induced by the pro-inflammatory cytokine TNF[alpha]. Biomaterials. 2009; 30(28):4907–4914. [PubMed: 19560813]

Lin S, et al. Influence of physical properties of biomaterials on cellular behavior. Pharm. Res. 2011; 28(6):1422–1430. [PubMed: 21331474]

Sawhney AS, Pathak CP, Hubbell JA. Bioerodible hydrogels based on photopolymerized poly(ethylene glycol)-co-poly(alpha-hydroxy acid) diacrylate macromers. Macromolecules. 1993; 26(4):581–587.

Young JL, Engler AJ. Hydrogels with time-dependent material properties enhance cardiomyocyte differentiation in vitro. Biomaterials. 2011; 32(4):1002–1009. [PubMed: 21071078]

Goldman SA. Progenitor cell-based treatment of the pediatric myelin disorders. Arch. Neurol. 2011; 68(7):848–856. [PubMed: 21403006]

Barker RA, et al. Stem cells and neurological disease. J. Neurol. Neurosurg. Psychiatry. 2003; 74(5): 553–557. [PubMed: 12700287]

Svendsen CN, Caldwell MA, Ostenfeld T. Human neural stem cells: isolation, expansion and transplantation. Brain Pathol. 1999; 9(3):499–513. [PubMed: 10416990]

Gupta N, et al. Neural stem cell engraftment and myelination in the human brain. Sci. Transl. Med. 2012; 4(155):155ra137.

Olanow CW, et al. A double-blind controlled trial of bilateral fetal nigral transplantation in Parkinson's disease. Ann. Neurol. 2003; 54(3):403–414. [PubMed: 12953276]

Trounson A, et al. Clinical trials for stem cell therapies. BMC Med. 2011; 9:52. [PubMed: 21569277]

Selden NR, et al. Central nervous system stem cell transplantation for children with neuronal ceroid lipofuscinosis. J. Neurosurg. Pediatr. 2013; 11(6):643–652. [PubMed: 23581634]

Luan Z, et al. Effects of neural progenitor cell transplantation in children with severe cerebral palsy. Cell Transplant. 2012; 21(Suppl. 1):S91–S98. [PubMed: 22507684]

Lo B, Parham L. Ethical issues in stem cell research. Endocr. Rev. 2009; 30(3):204–213. [PubMed: 19366754]

Su P, Loane C, Politis M. The use of stem cells in the treatment of Parkinson's disease. Insciences Journal. 2011; 1(3):136–156.

Pollard SM, et al. Adherent neural stem (NS) cells from fetal and adult forebrain. Cereb. Cortex. 2006; 16(Suppl. 1):i112–i120. [PubMed: 16766697]

Banerjee A, et al. The influence of hydrogel modulus on the proliferation and differentiation of encapsulated neural stem cells. Biomaterials. 2009; 30(27):4695–4699. [PubMed: 19539367]

Engler AJ, et al. Matrix elasticity directs stem cell lineage specification. Cell. 2006; 126(4):677–689. [PubMed: 16923388]

Georges PC, et al. Matrices with compliance comparable to that of brain tissue select neuronal over glial growth in mixed cortical cultures. Biophys. J. 2006; 90(8):3012–3018. [PubMed: 16461391]

Saha K, et al. Substrate modulus directs neural stem cell behavior. Biophys. J. 2008; 95(9):4426–4438. [PubMed: 18658232]

Seidlits SK, et al. The effects of hyaluronic acid hydrogels with tunable mechanical properties on neural progenitor cell differentiation. Biomaterials. 2010; 31(14):3930–3940. [PubMed: 20171731]

Teixeira AI, et al. The promotion of neuronal maturation on soft substrates. Biomaterials. 2009; 30(27):4567–4572. [PubMed: 19500834]

Elkin BS, Ilankovan A, Morrison B. Age-dependent regional mechanical properties of the rat hippocampus and cortex. J. Biomech. Eng. 2010; 132(1)

Ambati J, Rankin SE. Reaction-induced phase separation of bis(triethoxysilyl)ethane upon sol–gel polymerization in acidic conditions. J. Colloid Interface Sci. 2011; 362(2):345–353. [PubMed: 21788023]

Lee JW, et al. Synthesis and characterization of thermosensitive chitosan copolymer as a novel biomaterial. J. Biomater. Sci. Polym. Ed. 2004; 15(8):1065–1079. [PubMed: 15461190]

Jin N, et al. Tuning of Thermally induced sol-to-gel transitions of moderately concentrated aqueous solutions of doubly thermosensitive hydrophilic diblock copolymers poly(methoxytri(ethylene glycol) acrylate)-b-poly(ethoxydi(ethylene glycol) acrylate-co-acrylic acid). J. Phys. Chem. B. 2012; 116(10):3125–3137. [PubMed: 22352399]

He S, et al. Injectable biodegradable polymer composites based on poly(propylene fumarate) crosslinked with poly(ethylene glycol)-dimethacrylate. Biomaterials. 2000; 21(23):2389–2394. [PubMed: 11055286]

Hudalla GA, Eng TS, Murphy WL. An Approach to modulate degradation and mesenchymal stem cell behavior in poly(ethylene glycol) networks. Biomacromolecules. 2008; 9(3):842–849. [PubMed: 18288800]

Burdick JA, et al. Controlled degradation and mechanical behavior of photopolymerized hyaluronic acid networks. Biomacromolecules. 2005; 6(1):386–391. [PubMed: 15638543]

Cayre M, Canoll P, Goldman JE. Cell migration in the normal and pathological postnatal mammalian brain. Prog. Neurobiol. 2009; 88(1):41–63. [PubMed: 19428961]

Gage FH. Mammalian neural stem cells. Science. 2000; 287(5457):1433–1438. [PubMed: 10688783]

Seaberg RM, Smukler SR, van der Kooy D. Intrinsic differences distinguish transiently neurogenic progenitors from neural stem cells in the early postnatal brain. Dev. Biol. 2005; 278(1):71–85. [PubMed: 15649462]

Yeh J, et al. Micromolding of shape-controlled, harvestable cell-laden hydrogels. Biomaterials. 2006; 27(31):5391–5398. [PubMed: 16828863]

Kuntz RM, Saltzman WM. Neutrophil motility in extracellular matrix gels: mesh size and adhesion affect speed of migration. Biophys. J. 1997; 72(3):1472–1480. [PubMed: 9138592]

Chung C, et al. The influence of degradation characteristics of hyaluronic acid hydrogels on in vitro neocartilage formation by mesenchymal stem cells. Biomaterials. 2009; 30(26):4287–4296. [PubMed: 19464053]

Chung C, Burdick JA. Influence of three-dimensional hyaluronic acid microenvironments on mesenchymal stem cell chondrogenesis. Tissue Eng. A. 2009; 15(2):243–254.

Muir D. Metalloproteinase-dependent neurite outgrowth within a synthetic extracellular matrix is induced by nerve growth factor. Exp. Cell Res. 1994; 210(2):243–252. [PubMed: 8299723]

Stabenfeldt SE, et al. Biomimetic microenvironment modulates neural stem cell survival, migration, and differentiation. Tissue Eng. A. 2010; 16(12):3747–3758.

Bonneh-Barkay D, Wiley CA. Brain extracellular matrix in neurodegeneration. Brain Pathol. 2009; 19(4):573–585. [PubMed: 18662234]

Chodobski A, et al. Early neutrophilic expression of vascular endothelial growth factor after traumatic brain injury. Neuroscience. 2003; 122(4):853–867. [PubMed: 14643756]

Fainstein N, Cohen ME, Ben-Hur T. Time associated decline in neurotrophic properties of neural stem cell grafts render them dependent on brain region-specific environmental support. Neurobiol. Dis. 2013; 49:41–48. [PubMed: 22910454]

Riquelme PA, Drapeau E, Doetsch F. Brain microecologies: neural stem cell niches in the adult mammalian brain. Philos. Trans. R. Soc. Lond. B Biol. Sci. 2008; 363(1489):123–137. [PubMed: 17322003]

Taipale J, Keski-Oja J. Growth factors in the extracellular matrix. FASEB J. 1997; 11(1):51–59. [PubMed: 9034166]

Shu XZ, et al. Synthesis and evaluation of injectable, in situ crosslinkable synthetic extracellular matrices for tissue engineering. J. Biomed. Mater. Res. A. 2006; 79A(4):902–912. [PubMed: 16941590]

Shu XZ, et al. Attachment and spreading of fibroblasts on an RGD peptide-modified injectable hyaluronan hydrogel. J. Biomed. Mater. Res. A. 2004; 68A(2):365–375. [PubMed: 14704979]

Shu XZ, et al. Disulfide cross-linked hyaluronan hydrogels. Biomacromolecules. 2002; 3(6):1304–1311. [PubMed: 12425669]

Bellail AC, et al. Microregional extracellular matrix heterogeneity in brain modulates glioma cell invasion. Int. J. Biochem. Cell Biol. 2004; 36(6):1046–1069. [PubMed: 15094120]

Rauch U. Extracellular matrix components associated with remodeling processes in brain. Cell. Mol. Life Sci. 2004; 61(16):2031–2045. [PubMed: 15316653]

Ruoslahti E. Brain extracellular matrix. Glycobiology. 1996; 6(5):489–492. [PubMed: 8877368]

Chojnacki A, Weiss S. Production of neurons, astrocytes and oligodendrocytes from mammalian CNS stem cells. Nat. Protoc. 2008; 3(6):935–940. [PubMed: 18536641]

Kazanis I, et al. Quiescence and activation of stem and precursor cell populations in the subependymal zone of the mammalian brain are associated with distinct cellular and extracellular matrix signals. J. Neurosci. 2010; 30(29):9771–9781. [PubMed: 20660259]

Bischofs IB, Schwarz US. Cell organization in soft media due to active mechanosensing. Proc. Natl. Acad. Sci. 2003; 100(16):9274–9279. [PubMed: 12883003]

Lampe KJ, et al. Effect of macromer weight percent on neural cell growth in 2D and 3D nondegradable PEG hydrogel culture. J. Biomed. Mater. Res. A. 2010; 94(4):1162–1171. [PubMed: 20694983]

Keung AJ, et al. Soft microenvironments promote the early neurogenic differentiation but not self-renewal of human pluripotent stem cells. Integr. Biol. 2012; 4(9):1049–1058.

Balgude AP, et al. Agarose gel stiffness determines rate of DRG neurite extension in 3D cultures. Biomaterials. 2001; 22(10):1077–1084. [PubMed: 11352088]

Conti L, et al. Niche-independent symmetrical self-renewal of a mammalian tissue stem cell. PLoS Biol. 2005; 3(9):e283. [PubMed: 16086633]

Song H, Stevens CF, Gage FH. Astroglia induce neurogenesis from adult neural stem cells. Nature. 2002a; 417(6884):39–44. [PubMed: 11986659]

Song HJ, Stevens CF, Gage FH. Neural stem cells from adult hippocampus develop essential properties of functional CNS neurons. Nat. Neurosci. 2002b; 5(5):438–445. [PubMed: 11953752]

Noble M, et al. Precursor cell biology and the development of astrocyte transplantation therapies: lessons from spinal cord injury. Neurotherapeutics. 2011; 8(4):677–693. [PubMed: 21918888]

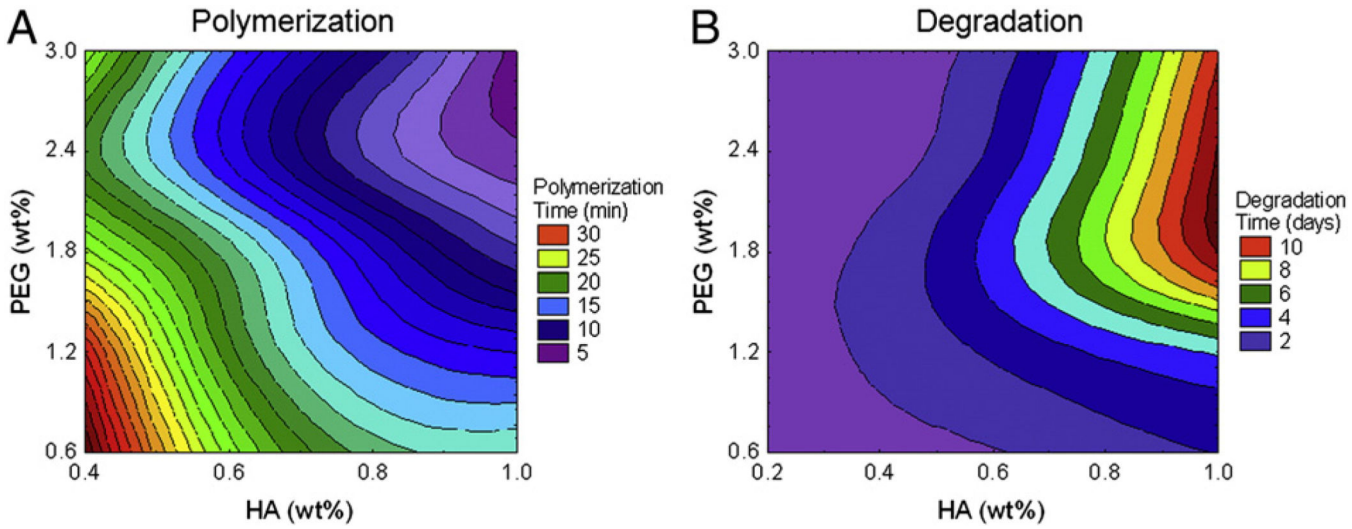

Figure 1.

Hydrogel physical properties. Polymerization and degradation rates for hydrogels were determined in vitro. A: Polymerization rate was measured in minutes. Time to polymerization decreased (purple contours) as HA and PEG concentrations both increased. B: Degradation rate of hydrogels submerged in hyaluronidase solution was measured in days. Hydrogels with greater amounts of total polymer took longer to degrade (red contours); at higher PEG contents (1.8% to 3.0%), degradation was dependent on the HA content of the hydrogel. HA: hyaluronic acid, PEG: poly(ethylene glycol), wt.%: percent weight by volume of polymer in final hydrogel formulation.

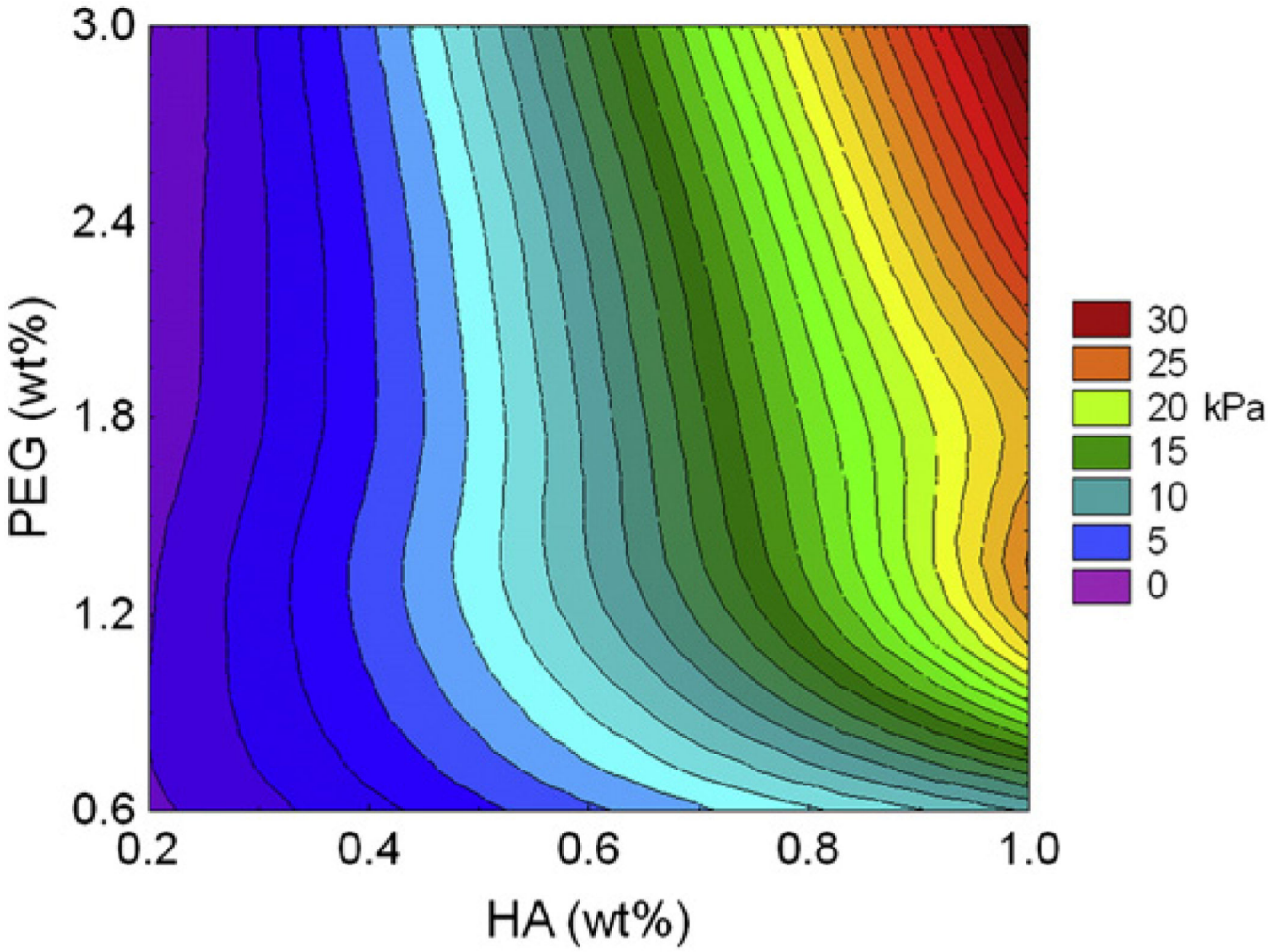

Figure 2.

Hydrogel mechanical properties. Compressive modulus was measured for all 25 HA and PEG hydrogel formulations. Hydrogels with the lowest compressive modulus were those containing 0.2% HA and higher concentrations of PEG, as indicated by the purple contours. The highest compressive modulus was measured in the 1.0% HA and 3.0% PEG hydrogel, as indicated by the red colored contour.

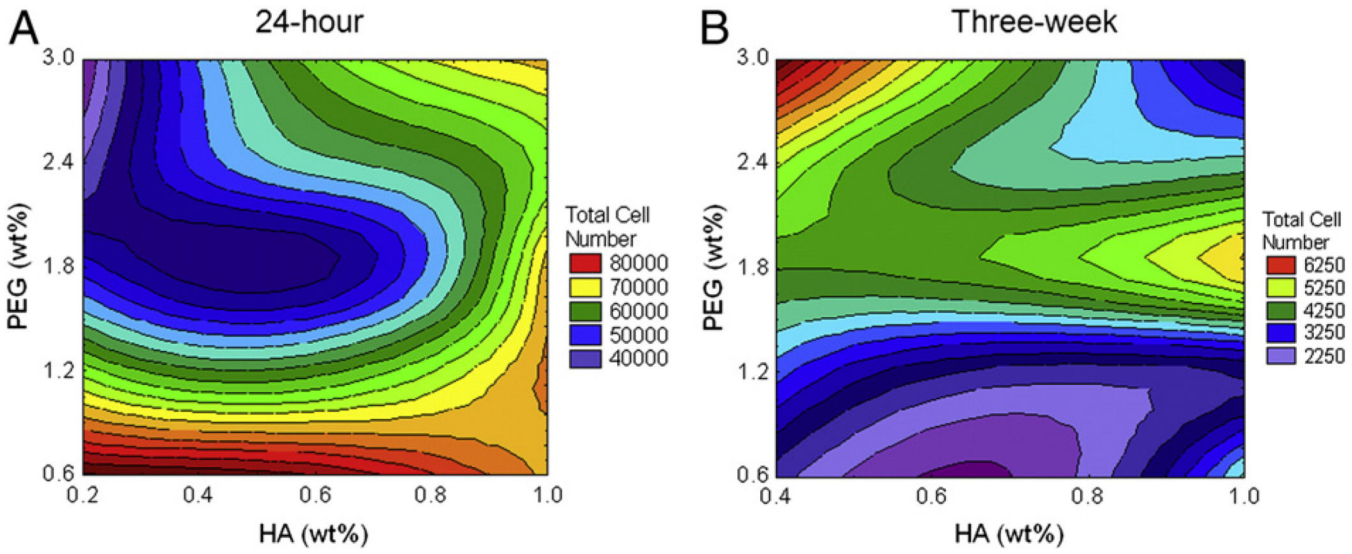

Figure 3.

Presence of fNPC at 24 h and three weeks. The total number of fNPC was determined at 24 h (A) and at three weeks (B) post-encapsulation. A. Measures indicated hydrogels with lower PEG content have increased survival at 24 h. Survival decreased as PEG content increased, mostly at lower concentrations of HA (purple and blue contours). B. Long-term cell numbers indicated that hydrogels with lower amounts of HA, but higher amounts of PEG had the greatest number of cells (red and yellow contours). Generally, hydrogels with lower concentrations of PEG had the lowest cell numbers at three weeks post-encapsulation, regardless of HA. Note that the plating density of the three week studies was half that of the 24 h studies, thus direct comparisons cannot be made between these two time-points.

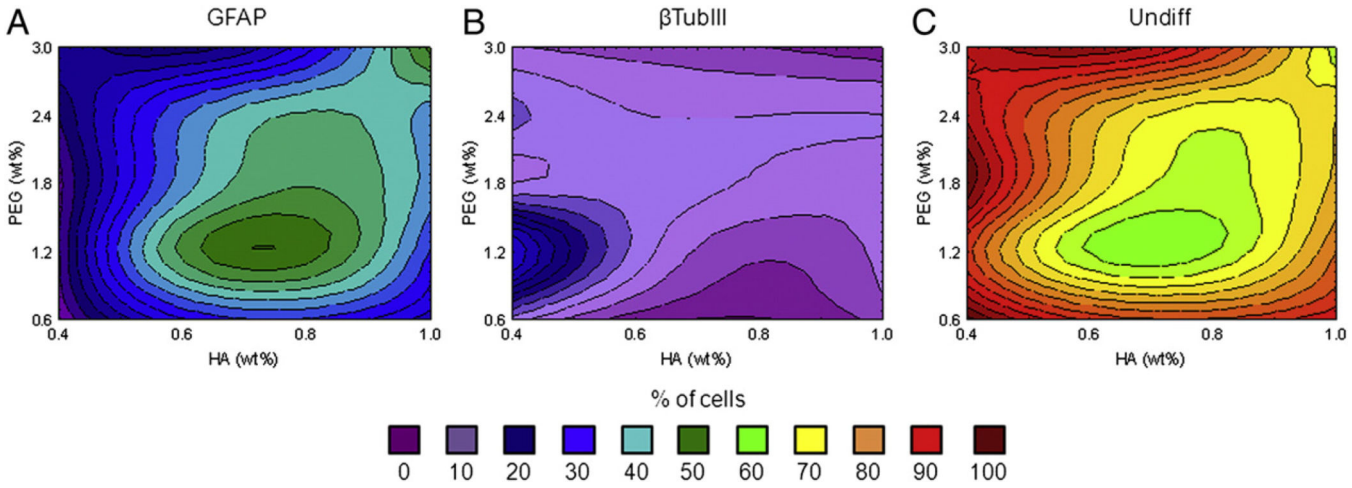

Figure 4.

fNPC differentiation. Differentiation of fNPC was assessed at three weeks post-encapsulation. A. When differentiation occurred, most cells were positive for GFAP, particularly in hydrogels with 0.6% and 0.8% HA and 1.2% PEG (green contours). B. Neuronal differentiation, as indicated by βTubIII immunoreactivity, was low and found primarily at 0.4% HA and 1.2% PEG (blue contours). C. The majority of fNPC were not positive for either βTubIII or GFAP, indicating they probably remained undifferentiated. Undiff: undifferentiated cells (GFAP−/βTubIII−).

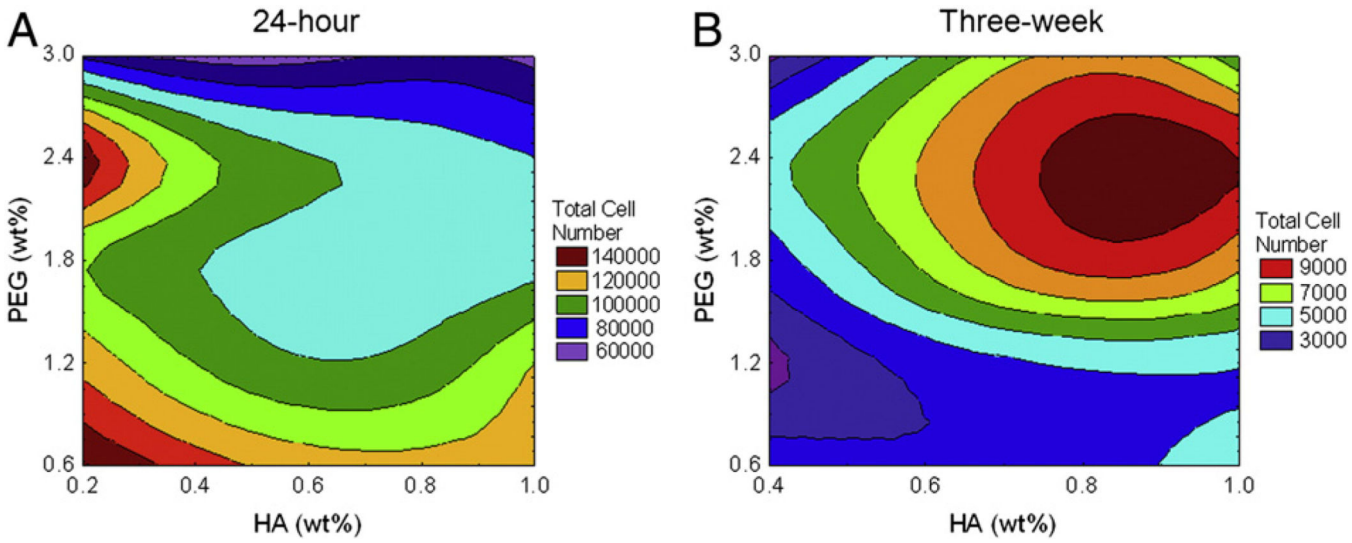

Figure 5.

Presence of aNPC at 24 h and three weeks. Total remaining aNPC numbers were determined at 24 h (A) and at three weeks (B) post-encapsulation. A. At 24-hours, survival of aNPC was best at lower concentrations of HA and PEG, although there was an increase in survival at 0.2% HA and 2.4% PEG (red contours). B. Analysis of aNPC cell numbers after three weeks of hydrogel encapsulation indicated aNPC were present in greater numbers in hydrogels with higher polymer content. Adult-NPC cell numbers were optimal at 0.8% and 1.0% HA with 2.4% PEG (red contour). Note that the plating density of the three week studies was half that of the 24 hour studies, thus direct comparisons cannot be made between these two time-points.

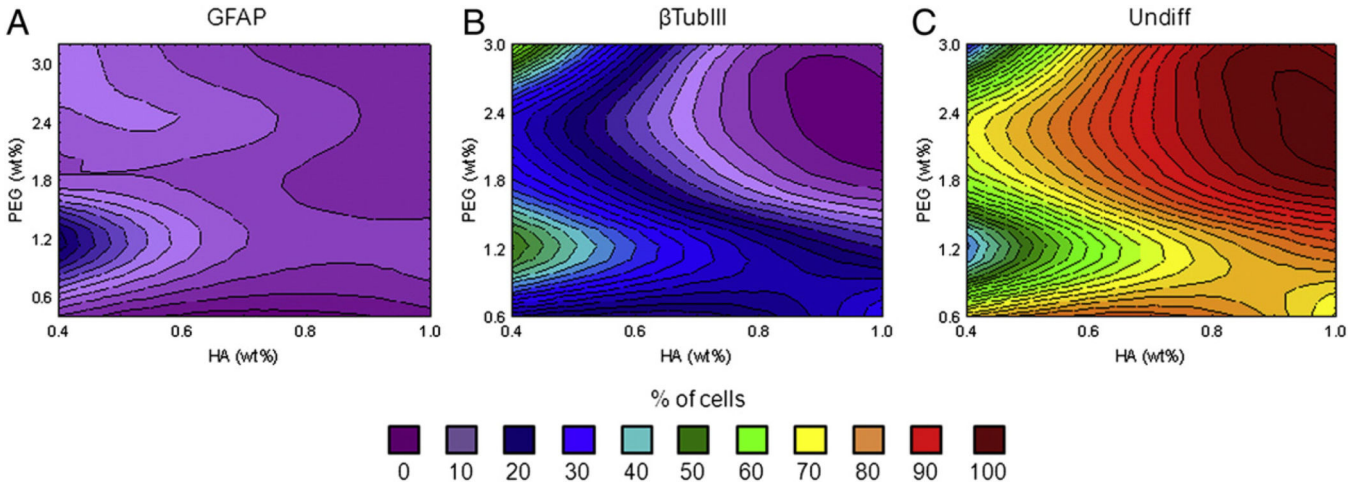

Figure 6.

aNPC differentiation. Differentiation of aNPC was assessed at three weeks post-encapsulation. A. Only a small population of aNPC differentiated to a glial lineage, as indicated by GFAP immunoreactivity (blue contours). B. The majority of differentiated cells adopted a neuronal fate, suggested by βTubIII immunoreactivity. Note the strong presence of green and blue contours, suggesting up to 40% of cells were βTubIII-positive. Increased differentiation was seen in hydrogels with 0.4% HA and 1.2% PEG, for both cell types assessed. C. Similar to fNPC, the majority of aNPC were neither βTubIII nor GFAP positive, suggesting that they likely remained undifferentiated at three weeks.

Table 1

Matrix of 25 hydrogels studied. Final hydrogel formulations based on the HA-to-PEG ratio were designated by the letters A–Y. For example, the hydrogel identified as formulation “M” had a final polymer concentration of 0.6%(w/ v) HA and 1.8%(w/v) PEG. HA: hyaluronic acid, PEG: poly(ethylene glycol), wt%: percent weight by volume of polymer in final hydrogel formulation.

		HA (wt%)				
		0.2	**0.4**	**0.6**	**0.8**	**1.0**
PEG (wt%)	3.0	U	P	K	F	A
	2.4	V	Q	L	G	B
	1.8	W	R	M	H	C
	1.2	X	S	N	I	D
	0.6	Y	T	O	J	E

Table 2

Brain tissue mechanical properties. Mean compressive moduli of brain tissue samples from rodents of various ages and species.

Species	Age	Compressive modulus (±SEM)	N
Mouse	2–3 mo	3.48 ± 0.92 kPa	5
Rat	P7	2.02 ± 0.15 kPa	3
	2–3 mo	8.50 ± 1.22 kPa	3
	4 mo	9.71 ± 2.50 kPa	4

All tissues were harvested from female rodents and tested at room temperature. P: post-natal day; mo: months of age; kPa: kilopascals; SEM: standard error of the mean; N: number of samples.